

# Lab on a Chip

Accepted Manuscript



This is an *Accepted Manuscript*, which has been through the Royal Society of Chemistry peer review process and has been accepted for publication.

*Accepted Manuscripts* are published online shortly after acceptance, before technical editing, formatting and proof reading. Using this free service, authors can make their results available to the community, in citable form, before we publish the edited article. We will replace this *Accepted Manuscript* with the edited and formatted *Advance Article* as soon as it is available.

You can find more information about *Accepted Manuscripts* in the [Information for Authors](#).

Please note that technical editing may introduce minor changes to the text and/or graphics, which may alter content. The journal's standard [Terms & Conditions](#) and the [Ethical guidelines](#) still apply. In no event shall the Royal Society of Chemistry be held responsible for any errors or omissions in this *Accepted Manuscript* or any consequences arising from the use of any information it contains.

# A Microfluidic Dual-well Device for High-throughput Single-cell Capture and Culture

Ching-Hui Lin,<sup>a,c</sup> Yi-Hsing Hsiao,<sup>a,d</sup> Hao-Chen Chang,<sup>a,c</sup> Chuan-Feng Yeh,<sup>a</sup> Cheng-Kun He,

<sup>a,c</sup> Eric M. Salm,<sup>e</sup> Chihchen Chen,<sup>d</sup> Ing-Ming Chiu<sup>b,c,f\*</sup> and Chia-Hsien Hsu<sup>a,c,d\*</sup>

5 <sup>a</sup> Institute of Biomedical Engineering and Nanomedicine, National Health Research Institutes, Miaoli, Taiwan

<sup>b</sup> Institute of Cellular and Systems Medicine, National Health Research Institutes, Miaoli, Taiwan

<sup>c</sup> Ph.D. Program in Tissue Engineering and Regenerative Medicine, National Chung Hsing University, Taichung, Taiwan

<sup>d</sup> Institute of NanoEngineering and MicroSystems, National Tsing Hua University, Hsinchu, Taiwan

<sup>e</sup> Department of Bioengineering, University of Illinois at Urbana-Champaign, Urbana, 61801, Illinois, USA.

15 <sup>f</sup> Department of Internal Medicine, The Ohio State University, Columbus, 43210, Ohio, USA

*Key words:* Microfluidic, High-throughput, Microwell, Single cell, Cell proliferation, Stem cell differentiation

**Abstract**

*In vitro* culture of single cells facilitates biological studies by deconvoluting complications from cell population heterogeneity. However, there is still a lack of simple yet high-throughput method to perform single cell culture experiment. In this paper, we report the development and application of a microfluidic device with a dual-well (DW) design concept for high-yield single-cell loading (~77%) in large microwells (285 and 485  $\mu\text{m}$  in diameter) which allowed for cell spreading, proliferation and differentiation. The increased single-cell-loading yield is achieved by using sets of small microwells termed “capture-wells” and big microwells termed “culture-wells” according to their utilities for single-cell capture and culture respectively. This novel device architecture allows the size of the “culture” microwells to be flexibly adjusted without affecting the single-cell loading efficiency making it useful for cell culture applications as demonstrated by our experiments of KT98 mouse neural stem cell differentiation, A549 and MDA-MB-435 cancer cell proliferation, and a single-cell colony formation assay with A549 cells in this paper.

15

## Introduction

Research into cellular heterogeneity<sup>1-3</sup> has important implications for the treatment of human diseases. For example, pluripotent stem cells represent a powerful platform for modeling disease and hold promising potential in regenerative medicine, but robust differentiation of pluripotent stem cells has been difficult due to the functional heterogeneity of pluripotent stem cells.<sup>4</sup> In cancer cells, a small population of “cancer stem/initiating cells” are believed to be responsible for chemotherapy resistance.<sup>5</sup> Measuring cell-to-cell variability may deconvolute complex biological questions and provide new directions for fighting diseases.<sup>6-8</sup>

Analyzing individual cells, however is technically more challenging compared to measuring the averaged outcome from a cell population.<sup>9</sup> Such tasks are commonly performed with limiting dilution or fluorescence-activated cell sorting (FACS). Limiting dilution is based on placing diluted cell suspension in culture wells (*e.g.*, plastic well plates) to obtain one-cell-in-a-well events, and is widely used for single cell assays such as colony formation of cancer stem/initiating cells<sup>10</sup>. This method is convenient but low-throughput without using pipetting robot, because the maximum probability of single-cell event is under 37% according to the Poisson distribution<sup>11</sup>. FACS can overcome the Poisson distribution limitation and provide an alternative method to efficiently obtain single-cell events by sorting and placing

individual cells in well plates<sup>12</sup>. However, the high mechanical shear stress in FACS can damage cells and affect their downstream uses.<sup>13</sup> In addition, FACS is less prevalent in many laboratories due to its high machine-purchasing and operational cost.

Microfabricated devices have emerged as a useful tool for single-cell applications<sup>14, 15</sup>,  
5 based on ability to accurately manipulate single cells.<sup>16</sup> These miniaturized devices also allowed for high-throughput processing and reduced sample and reagent consumptions.<sup>13</sup> Recently, microfabricated devices have been utilized for capturing single cells for single cell analysis using microdroplets<sup>17, 18</sup>, dielectrophoresis<sup>19, 20</sup>, hydrodynamics<sup>21, 22</sup>, selective dewetting<sup>23, 24</sup>, mechanical techniques<sup>25-27</sup> and microwell array on different substrates<sup>16, 28</sup>. For  
10 cell-based applications that require culturing single cells, microdroplet-based methods represent a powerful means of obtaining larger numbers of microdroplets each containing a single cell. However it is difficult to change the medium inside the microdroplets, making it not suitable for applications where the initial medium need to be replaced during experiment. In addition cells encapsulated in microdroplets are not suitable for adherent cell culture due to  
15 the lack of a substrate for cell to attach and spread. One the other hand, trapping single cells in microwells is an attractive method to set up larger numbers of single cells for both adherent and suspension single-cell cultures due to its simplicity in device fabrication and operation as

they only require physical walls and simple manipulation (*e.g.*, by using flow or gravity) to load cells in compartmented spaces for subsequent culture and analysis<sup>16, 29, 30</sup>. However, in order to provide sufficient space for cell growth, the sizes of the microwells had to be made much larger (from 90 – 650  $\mu\text{m}$  in diameter or in side length) than that of a single cell, resulting in low single-cell events (ranging from 10 – 30%).<sup>29-32</sup> The decreased single-cell-loading efficiency in large microwells is due to the inherent limitation of the Poisson distribution also seen in conventional limiting dilution method<sup>33</sup>. This limitation was improved by using triangle-shaped microwells which were able to provide enlarged area for cell growth while maintain good single-cell loading efficiency (up to  $\sim 58\%$ ). However the enlarged area ( $\sim 3.5 - 6$  times of that of a single cell) in a microwell was insufficient for cells grow beyond two days.<sup>34</sup>

In this paper, we describe the concept and development of a microfabricated Dual-Well (DW) device which allows for high-efficient loading of single cells in large microwells whose size can be made significantly larger than a single cell for single-cell culture application. The increased efficiency of single-cell loading in large microwells is achieved by utilizing a novel concept of using small microwells to trap singles cells followed by using gravity to transfer the captured cells to large microwells for the cells to spread and grow during cell

culture. We report the characterization of the design and cell-loading operation parameters of the DW device and demonstrated the utilities of the DW device in cell proliferation, differentiation and a single-cell colony formation assay experiments with adult mouse brain neural stem/progenitor KT98 cells, as well as two cancer cell lines: A549 and MDA-MB-435.

5

## EXPERIMENTAL SECTION

### Device design and fabrication

The DW microfluidic devices were made of polydimethylsiloxane (PDMS) using soft lithography techniques.<sup>35</sup> Briefly, negative photoresist (SU-8, MicroChem, Newton, MA, USA) was photolithographically patterned on silicon wafers to create masters. The height of the SU-8 features was measured using a scanning laser profilometer (VK-X 100, KEYENCE, Japan). The masters were then used as molds, on which Sylgard 184 (Dow corning, USA) PDMS pre-polymer mixed with its crosslinker at 10:1 ratio was poured and allowed to cure in a conventional oven at 65°C for 3 hours. The cured PDMS replicas were peeled off from the molds. A puncher with 1.00 mm inner-diameter (Harris Uni-Core™, Ted Pella, USA) was used to punch inlet holes for the fluidic channel of the PDMS device. After a brief oxygen plasma treatment, the PDMS replicas were aligned, brought to contact and placed in an oven at 65 °C for 24 hours to achieve permanent bonding between the PDMS replicas.

### DW device preparation for single-cell capturing

Prior to cell experiment, the DW devices were filled with deionized water and soaked in a deionized water-filled container in a desiccator to remove air-bubbles in the microchannel. Subsequently, the degassed DW devices were exposed UV light to sterilize for 30 minutes. To



prevent immediate cell adhesion to the PDMS surface, 5% BSA (Bovine serum albumin, Bersing Technology, Taiwan) in 1x PBS was injected into microfluidic channel and incubated at 37 °C for 30 minutes<sup>36</sup>.

### **Cell culture and maintenance**

5 KT98 cells derived from F1B-TAg transgenic mouse brain<sup>37</sup> were used as a cell model in this study. In routine maintenance, KT98 cells were cultured in DMEM/F12 medium (Gibco, USA) with 10% fetal bovine serum (Hyclone Thermo, USA) and 1% anti-biotics (Glutamine-Penicillin-Streptomycin, Biowest, France) at 37 °C and 5% CO<sub>2</sub> in a humidified incubator. Cancer cell lines - human lung cancer A549 and melanoma MDA-MB-435 - were  
10 maintained in DMEM basal medium (Gibco, USA) with 10% fetal bovine serum (FBS, Biowest, France) and 1% anti-biotics. The cell cultures were passaged using a recombinant enzyme Accumax™ (Innovative cell technology, USA) under the manufacture's standard protocol at 70 – 80% confluence.

### **Single-cell capture and culture**

15 Prior to each cell-capture experiment, the cells were prestained with a membrane dye (DiIC12(3), BD Biosciences, USA) for 20 minutes for easy-identification of the cells in the DW device. For each single-cell capture experiment, 200 μL of KT98 cells at 2.2 – 2.5 x 10<sup>6</sup>

cells/mL concentration ( $4.4 - 5 \times 10^5$  cells) was loaded to a 200  $\mu$ L plastic pipette tip followed by inserting the tip to the device inlet hole to manually inject the cells into the microfluidic channel of the DW device. This operation step can quickly load cells into the microchannel to cover the area of capture-wells. A syringe run by a syringe pump (Harvard Apparatus, Harvard Bioscience, USA) was then connected to the inlet of the DW device via a Teflon tubing (poly(tetrafluorethylene), inner dia.: 0.51 mm, outer dia.: 0.82 mm, Ever Sharp Technology, Inc., Taiwan) to drive 20  $\mu$ L of the cell culture medium into the device at 3  $\mu$ L/min. During this step, the cells in the microchannel moved slowly and could settle into the captured-wells by gravitational force. Subsequently, the uncaptured cells were washed away from the device by using 300  $\mu$ L of the cell culture medium run at different flow rates of 200, 400, 600 and 800  $\mu$ L/min. Finally, the inlet and outlet holes were sealed with plugs, and the device was flipped upside down to transfer the captured-cells to the culture-wells by gravitational force (Figure 1B and 2A). The device was then placed in a standard cell culture incubator at 37 °C and 5% CO<sub>2</sub> for 6 – 7 days.

#### 15 **KT98 cells differentiation in DW devices**

Stem cell differentiation in DW device was achieved by replacing the culture medium with a differentiation medium (NeuroCult™ Differentiation Kit, STEMCELL Technologies, Canada)

1 day after seeding KT98 cells in 485  $\mu\text{m}$ -diameter culture-wells, using the following steps: 1) The plugs in the inlet and outlet holes were removed. 2) A differentiation medium loaded syringe was connected to the inlet hole via a Teflon tubing. 3) A syringe pump was used to inject the differentiation medium to the microchannel of DW device at slow flow rate of 1.8 mL/hr. 4) The inlet and outlet holes were resealed with the plugs and the device was placed into the cell culture incubator and cultured for 7 days. Then the cells were fixed with 4% paraformaldehyde (Alfa Aesar, USA) for 15 minutes at room temperature, washed three times with 1X PBS, permeabilized with 0.25% Triton X-100 (Sigma, USA) in 1X PBS for 10 minutes and washed three times again with 1X PBS. After blocking nonspecific binding with 1% BSA in PBST (PBS + 0.1% Tween-20), the cells were incubated with Microtubule-associated protein 2 (MAP2, MAB378, Millipore, USA) antibody in a 4°C refrigerator overnight. Subsequently, the cells were incubated with FITC-conjugated secondary antibody for 1 hour at room temperature. All cells were stained with DAPI to provide a counter staining.

#### 15 **A549 clonal culture for EGF promoted colony formation assay in DW devices**

In the EGF promoted colony formation assay, 200  $\mu\text{L}$  of A549 cells at a concentration of  $2.2 - 2.5 \times 10^6$  cells/mL was injected into the DW device manually, waited for 2 min for cells to

settle, and followed by injecting DMEM with 20% FBS and 1% anti-biotics into the microchannel immediately to wash off the excessive cells in the channel at a flow rate of 600  $\mu\text{L}/\text{min}$  for 30 sec. Subsequently, the inlet and outlet holes were sealed and the device was flipped upside down to obtain a single-cell in a culture-well. The device was then placed into a humidified incubator at 37 °C and 5%  $\text{CO}_2$  as described above. After 1 day of culture, one of the device (for the control experiment) was injected with 300  $\mu\text{L}$  of DMEM containing 10% FBS and 1% anti-biotics to replace the original medium. The other device (for the EGF treatment experiment) was injected with 300  $\mu\text{L}$  of DMEM containing 10% FBS, 1% anti-biotics and 200 ng/mL of epithelial growth factor (EGF, PeproTech, USA) to replace the original medium. For both devices the medium was replaced with fresh medium every 3 days. After 7 days of culture, the cells were imaged to assess the colony forming efficiency. Colonies with cell number larger than 15 cells in a culture well were scored as cell colonies.

### **Cell imaging**

All cell images were obtained using an inverted microscope (Nikon Ti-E inverted fluorescence microscope, Japan) with an attached charge-coupled device (Retiga-4000DC, Qimaging, Canada) and a control software (NIS-Elements Ar, Nikon, Japan).

### **Statistical analyses**

All experiments were performed in triplicate or quadruplicate, and the data are presented as means  $\pm$  standard deviation (SD). One-way analysis of variance (ANOVA) and Student's t-test was used for the comparison of each group. In Figure 3 to 6, the statistical significance was indicated with an asterisk was used to denote statistical significance at \*  $p < 0.05$ , \*\*  $p < 0.01$

5 and \*\*\*  $p < 0.001$  on figures.

## Results

### Device design and operation

As shown in Figure 1, the Dual-Well device consists of a microchannel with two sets of microwell arrays (each set contains 470 wells in an area of  $10.65 \times 7.7 \text{ mm}^2$ ) on its ceiling and floor. The use of microwells whose sizes are close to that of a single cell have been used to trap single cells at high efficiencies<sup>16, 28, 38</sup>. We have successfully adapted this method to achieve high-efficiency single-cell trapping in our DW device. The two sets of the microwells were designed in different sizes with each microwell in one set being  $25 \mu\text{m}$  in diameter and  $26 \text{ or } 30 \pm 1 \mu\text{m}$  in depth ( $0.013 \text{ nL}$  for each  $26 \mu\text{m}$  well,  $0.015 \text{ nL}$  for each  $30 \mu\text{m}$  well) and in the other set being  $285 \text{ or } 485 \mu\text{m}$  in diameter and  $300 \pm 15 \mu\text{m}$  in depth ( $\sim 20 \text{ nL}$  for each  $285 \mu\text{m}$  well,  $\sim 55 \text{ nL}$  for each  $485 \mu\text{m}$  well) (Figure S1). The microchannel height between the microwell sets was  $200 \mu\text{m}$ , resulting in a total volume of  $60 \mu\text{L}$  for the DW device. The footprint of the Dual-Well device is  $12.75 \times 20.25 \text{ mm}^2$ . The positions of capture- and culture-wells are arranged in a way that from the top-view angle, the position of each cell-capture well is located at the center a cell-culture well. The operation of the DW device involves the following steps (Figure 2A): 1) A cell suspension is injected into the microfluidic channel with a manual pipette while the device is placed at its “capture position” in which the

capture-wells are on the channel's floor and culture-wells are on the ceiling. 2) A tubing connected to a culture medium-loaded syringe is insert into the microchannel's inlet to inject medium to "sweep" the cells at a slow flow rate controlled by a syringe pump. This step increases the probability of cell ducking in the capture wells (Figure 2C, Video S1). 3) 5 Subsequently, the flow rate is increased to wash away the uncaptured cells (Figure 2D, Video S2). 4) And finally, the inlet holes are plugged after removing the tubing, and the DW device is gently flipped to its "culture position" in which the capture-wells are now on the channel's ceiling and culture-wells are on the floor, allowing the captured-cells to fall off from the capture-wells to the culture-wells by gravity (Figure 2E, Video S3). The loading procedure 10 takes about 8 – 9 minutes to perform and once flipped the device can be immediately placed in a humidified container (e.g., petri-dish) and placed in a conventional cell culture incubator for subsequent cell culture and experiments. Note that the DW device can be straightforwardly operated with conventional syringe pump, tissue culture incubator and microscopes making it highly adaptable to biological laboratories.

15

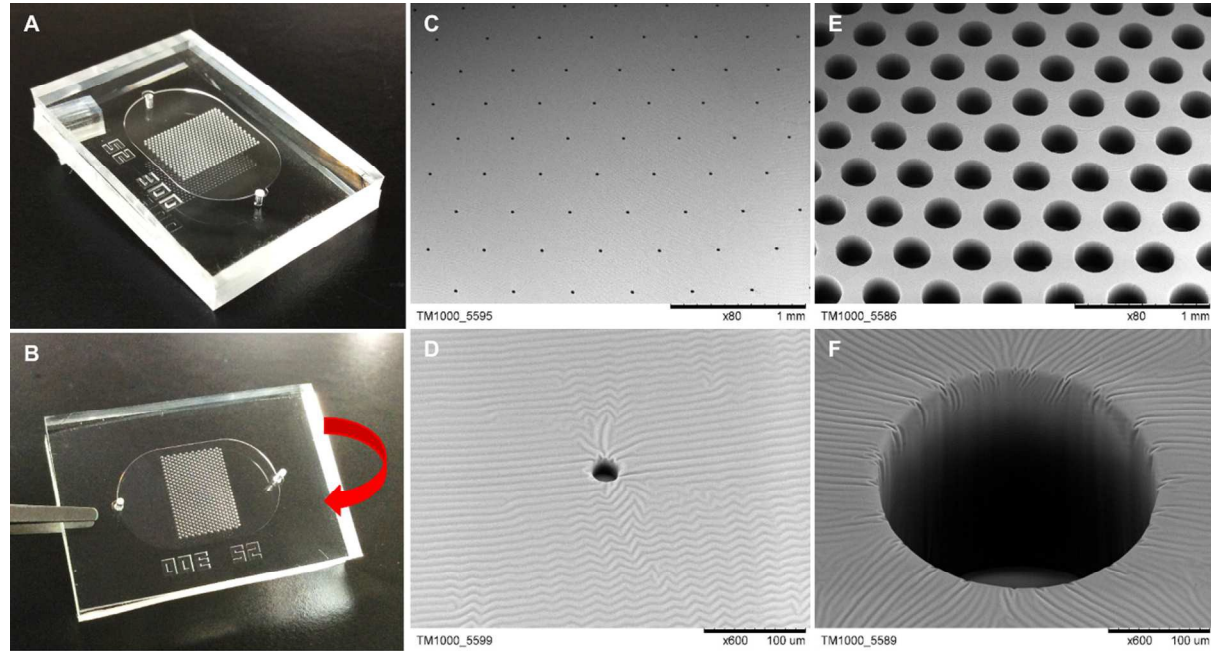


**Figure 1. Photograph and SEM images of dual-well device.** (A) Appearance of the DW device in PDMS. (B) Single-cells in capture-wells is transferred to culture-wells by the flipping the device. (C-D) SEM images of capture-wells with 25 μm diameter and 30 ± 1 μm depth. (E-F) SEM images of culture-wells with 285 μm diameter and 300 ± 15 μm depth.



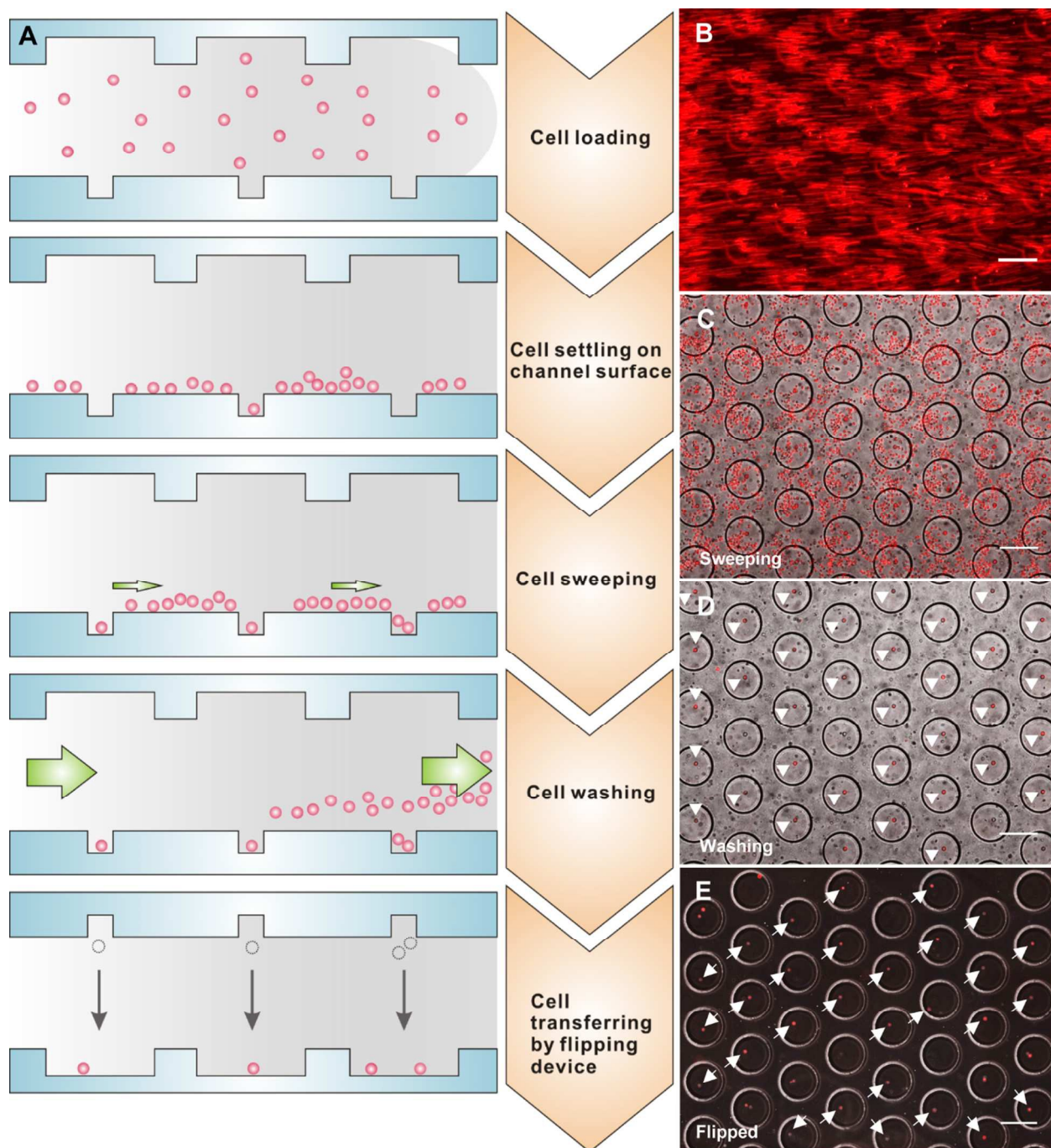


**Figure 2. Schematic illustration of DW device operation procedure.** (A) Flow diagram of DW device operation steps including cell loading, sweeping, washing and transferring. (B) A long exposure image (90 seconds) taken in sweeping step, showing 89.87% of the channel

floor area was covered by the trajectories of fluorescently (DiI membrane dye) labeled KT98 cells. (C) Cell capture efficiency in capture-wells is enhanced by moving cells with a slow flow. (D) Uncaptured cells are removed from the microchannel by washing. (E) Cells in capture-wells are transferred to culture-wells by flipping the device. Scale bar: 300  $\mu\text{m}$ .

5

### Single-cell capture efficiency of DW device with KT98 cells

For a cell to settle into a microwell, the projected area of the cell needs to overlap with that of the microwell. Therefore putting more cells in the microchannel could in theory increase the efficiency of microwell cell capture by increasing the probability of having cells on top of the microwells. However increasing cell density could also increase cell clustering during cell suspension preparation and device operation which decreases single cell capture yield. To avoid using very high-density cell suspension while keeping cell capture at high efficiency, a cell “sweeping” procedure is used in our system. We found that using 20  $\mu\text{L}$  of medium driven at 3  $\mu\text{L}/\text{min}$  was fast enough to move the cells in the microchannel, but slow enough to allow the cells to settle into the capture-wells (Video S1). Using KT98 cell suspension at 2.2 - 2.5 x 10<sup>6</sup> cells/mL density, we observed minimal cell clustering and more than 99% of the capture wells were occupied by cells (Figure 2C and 3A). We also tested the effect of washing flow rate on cell retention in the capture-wells and found that only a portion of the capture-wells (26  $\mu\text{m}$  in depth) lost their initially loaded cells with no significant difference (ranged from 81 – 85%) among the four tested flow rates after washing step (Figure 3B). However the washing flow rate did have a prominent effect on the number of cells being captured in a capture-well as shown by the cell loading result in culture-wells after flipping device; the

highest single-cell loading efficiency in culture-wells was obtained with 600 or 800  $\mu\text{L}/\text{min}$  washing flow rate (Figure 4G), indicating more capture wells were loaded with one cell with the 600 or 800  $\mu\text{L}/\text{min}$  flow rate (note that the flipping step only resulted less than 2% cell loss (Figure 3A)). Altogether, our results showed that with the current microwell dimensions, multiple single cells could stack in a capture well and being washed out from the well depending on the washing flow rate used, and the highest single-cell loading efficiency in culture wells of KT98 cells ( $77.31 \pm 3.70\%$ ) could be obtained by using the 600  $\mu\text{L}/\text{min}$  washing flow rate with the 26  $\mu\text{m}$  deep capture-wells. Additionally, to understand whether the single-cell capture ratio could be affected by the depth of the capture-wells, we conducted the single-cell capture efficiency test with another device which has deeper capture-wells (30  $\mu\text{m}$ ). The results showed the cell capture efficiency after sweeping was not affected by the depth difference between the shallow (26  $\mu\text{m}$ ) and deep (30  $\mu\text{m}$ ) capture-wells; both reached a very high efficiency ( $> 99\%$ ) after sweeping (Figure 3A). However, for the washing step the deep wells resulted in lower cell losses at the four flow rates (86.42% – 92.13% cell retention) than the shallow wells (80.94% – 85.16%, Figure 3B). However the single-cell ratio in cell-loaded culture-wells was decreased (from 89 – 92% to 64 – 75%, Figure 3C and 4D) when the capture-well depth was increased (26 to 30  $\mu\text{m}$ ), resulting in the reduction of single-cell ratio

in the total culture-wells (70 – 71% to 58 – 66%, Figure 3D). The highest single-cell ratio in total culture-wells ( $66.81 \pm 4.15\%$ ) was obtained by using 200  $\mu\text{L}/\text{min}$  washing flow rate with 30  $\mu\text{m}$ -deep capture-wells.

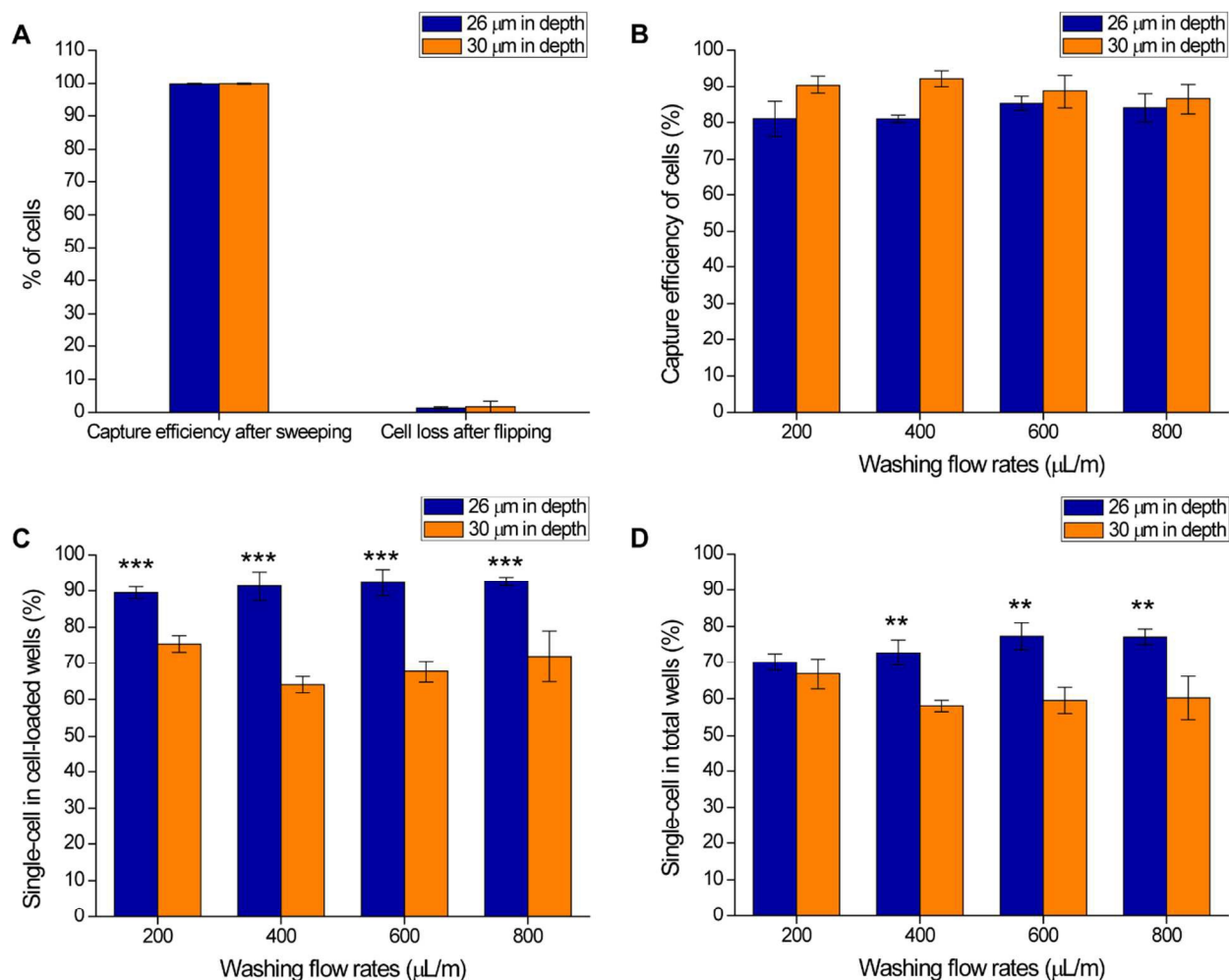


**Figure 3. KT98 cell loading efficiency after different operation steps in DW device with**

**26 and 30 μm-deep capture-wells. (A)** Efficiency of cell capture in capture-wells after

sweeping was reaching to 99.9%, and the cell loss after transferring the captured cells from

5 capture-wells to culture-wells was less than 2% of the both capture-well depth. (B) Cell

capture efficiency of in 30 μm-deep capture-wells (90.39%, 92.13%, 88.51% and 86.42%)

was higher than 26 μm-deep (80.97%, 80.94%, 85.16% and 83.97%) after washing at the flow

rates of 200, 400, 600 and 800 μL/min. (C) Frequency of single-cell event in cell-loaded

culture wells. The single-cell events of 26  $\mu\text{m}$ -deep capture-wells were significantly higher than 30  $\mu\text{m}$ -deep at the four flow rates. (D) Frequency of single-cell event in total culture wells. The single-cell events of 26  $\mu\text{m}$ -deep capture-wells were also higher than 30  $\mu\text{m}$ -deep.

Note, the highest single-cell event in total culture-wells (77%) was at using 26  $\mu\text{m}$ -deep

5 capture-wells with 600  $\mu\text{L}/\text{min}$  ratio washing flow rate. Each experiment was performed in triplicate.

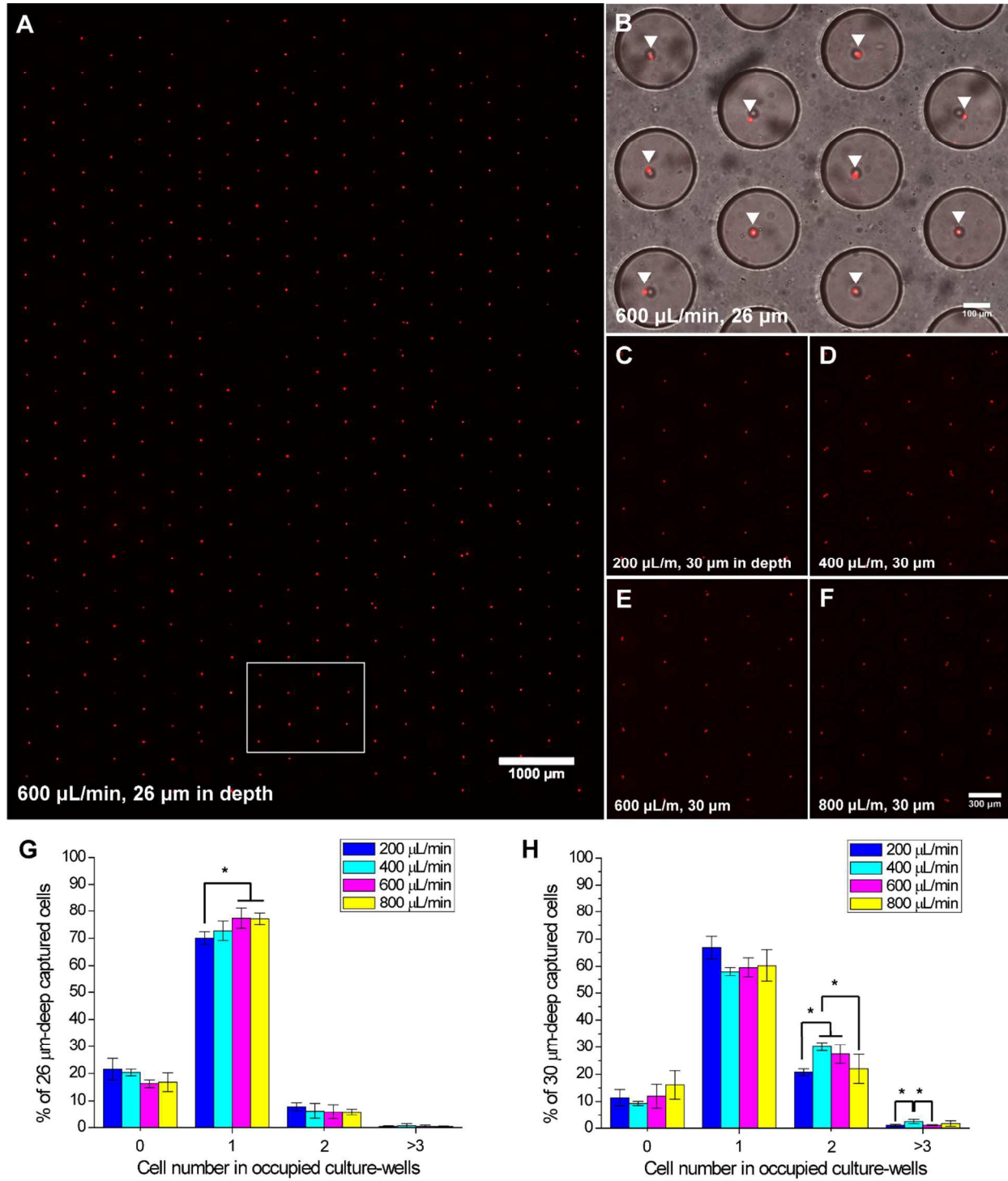


**Figure 4. Representative images of cells and cell number in cell-occupied culture-wells after flipping device (with the 26 and 30 µm-deep capture-wells). (A) A stitched image**



containing all 470 culture-wells (with 600  $\mu\text{L}/\text{min}$  washing flow rate). Scale bar: 1000  $\mu\text{m}$ . (B)

Enlarged overlapped images from the rectangle area of stitched image showing each

culture-well contains one single-cell. Arrowhead indicates the single-cells in culture-wells.

(C-F) Representative images from experiments using four different washing flow rates of 200,

5 400, 600 and 800  $\mu\text{L}/\text{min}$ . Higher frequency of 2 or >3 cell-occupied culture-wells were

shown in the result of experiment using 400  $\mu\text{L}/\text{min}$  washing flow rate. (G-H) Cell number in

cell occupied-culture-wells at four washing flow rates. The single cell ratio was higher using

600 or 800  $\mu\text{L}/\text{min}$  washing flow rates (77.31% and 77.09%, respectively), and lowest using

200  $\mu\text{L}/\text{min}$  washing flow rates (70.07%) with 26  $\mu\text{m}$ -deep capture-wells. (H) The highest

10 ratio-single event in total culture-wells (66.81%) was obtained by using 200  $\mu\text{L}/\text{min}$  washing

flow rate with 30  $\mu\text{m}$ -deep capture-wells.

### Single-cell capture efficiency of different cell types

To investigate the applicability of DW device to other cell types, two additional cell line cells - human lung cancer A549 (Figure S2) and melanoma MDA-MB-435 (Figure S3) - were tested with the DW device using 3  $\mu\text{L}/\text{min}$  sweeping flow rate and 600  $\mu\text{L}/\text{min}$  washing flow rate with the 26  $\mu\text{m}$  deep capture-wells according to the optimal KT98 single-cell loading results. The results showed that the ratio of cell-occupied capture wells after sweeping and washing is cell-type dependent (ranged from  $67.80 \pm 11.38\%$  –  $85.16 \pm 1.91\%$ , Figure 5B). Cell loss after the flipping step was low for all cell types of KT98, A549 and MDA-MB-435 (all less than 2%, Figure 5C). Interestingly, most of the cell-loaded culture-wells contained only a single cell in each well for all the three cell types ( $89.89\%$  –  $92.98\%$ ). All together our result showed that the DW device had good single-cell loading efficiencies in culture-well for KT98 and MDA-MB-435 (more than 76%, Figure 5D), except for A549 ( $61.63 \pm 7.47\%$ ). To improve the single-cell loading efficiency in the culture-well of different sizes of cells, we used the same depth but wide (from 25  $\mu\text{m}$  to 30  $\mu\text{m}$  in diameter) capture-well for cell trapping. Results showed the significant increment of single-cells loading efficiency ( $61.63\%$  to  $76.03\%$ , Figure 5E) was obtained using the A549 cell model. This result indicated that the efficiency of single-cell loaded in the culture-well was relied on the relationship between the sizes of cells and capture-wells.

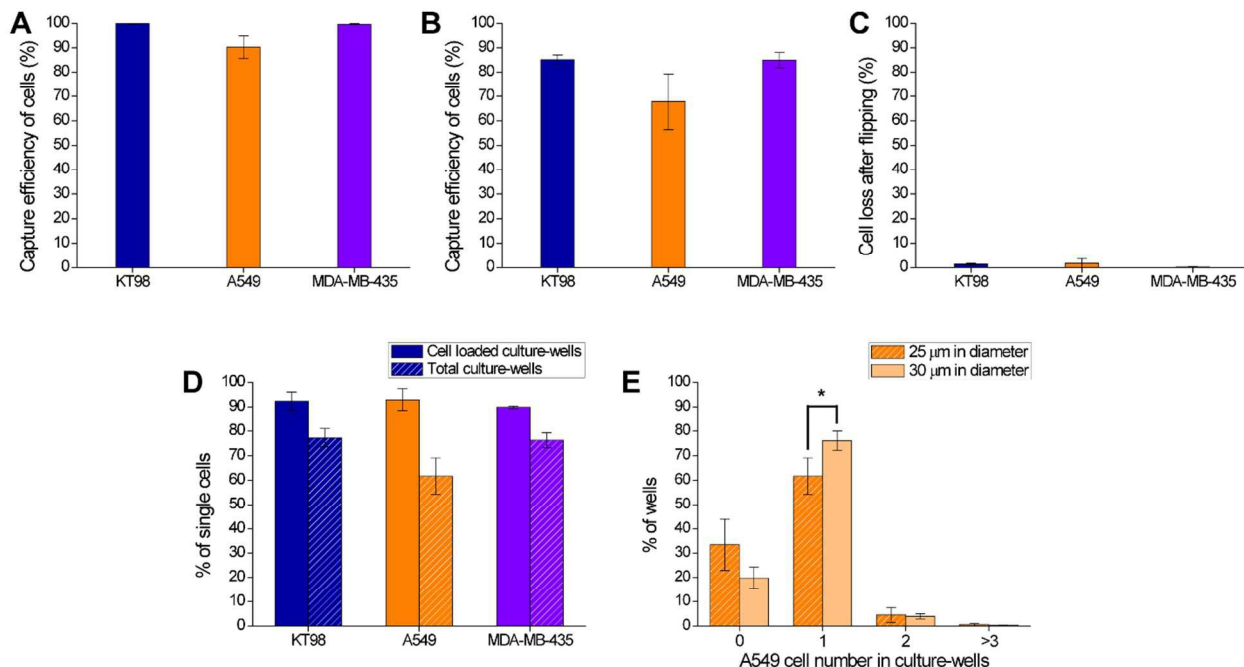


**Figure 5. KT98, A549 and MDA-MB-435 cell loading efficiency with 600  $\mu\text{L}/\text{min}$  washing**

**flow rate and 26  $\mu\text{m}$  deep capture-wells.** (A) Capture efficiency of KT98 and MDA-MB-435

cells were higher than 99%, but 90.21% of A549 after sweeping. (B) Efficiency of KT98,

5 A549 and MDA-MB-435 cells capture in capture-wells after washing at the flow rate of 600

$\mu\text{L}/\text{min}$ . (C) Cell loss was less than 2% of all the three cell types after device flipping. (D) The

single-cell ratio in total culture-wells (slash bar) of KT98, A549 and MDA-MB-435 cells was

77.31%, 61.63% and 76.31%, respectively. (E) The single cell capture efficiency of A549 was

significantly increased from 61.63% to 76.03% when the depth of capture-well was increased

10 to 30  $\mu\text{m}$ . Each experiment was performed in triplicate.

### Single-cell proliferation and stem cell differentiation in the microwells of DW device

The applicability of DW device for cell proliferation was demonstrated with KT98 and A549 cells. The enlarged culture-wells provided sufficient surface area for the cells to attach and spread as well as adequate medium volume for cell proliferation for up to one week. Using

5 culture-wells of a 285  $\mu\text{m}$  diameter ( $\sim 20$  nL), single KT98 and A549 cells were able to divide to 6 – 8 cells from a single cell in the microwell and form a colony (Figure 6A-D) after 6 – 7 days of culture in the device. On the other hand, the large culture wells and medium exchangeable feature of DW device allowed us to demonstrate its utility in stem cell differentiation which require long cell culture times ranging from 7 – 16 days for embryonic

10 stem cells <sup>39, 40</sup> and 7 – 21 days for neural stem cells <sup>41</sup> As shown in Figure 6E – G, after replacing the culture medium with differentiation medium in DW device one day after cell loading, a single KT98 cell in culture well (285  $\mu\text{m}$  in diameter) divided to 6 cells and exhibited neurite morphology specific to neuronal cells. As shown in Figure 6H – K, successful differentiation of KT98 from single KT98 cell was also verified by

15 immunocytochemistry staining of microtubule-associated protein 2 (MAP2) - a neuronal lineage protein marker which is involved in microtubule assembly essential for neuritogenesis.

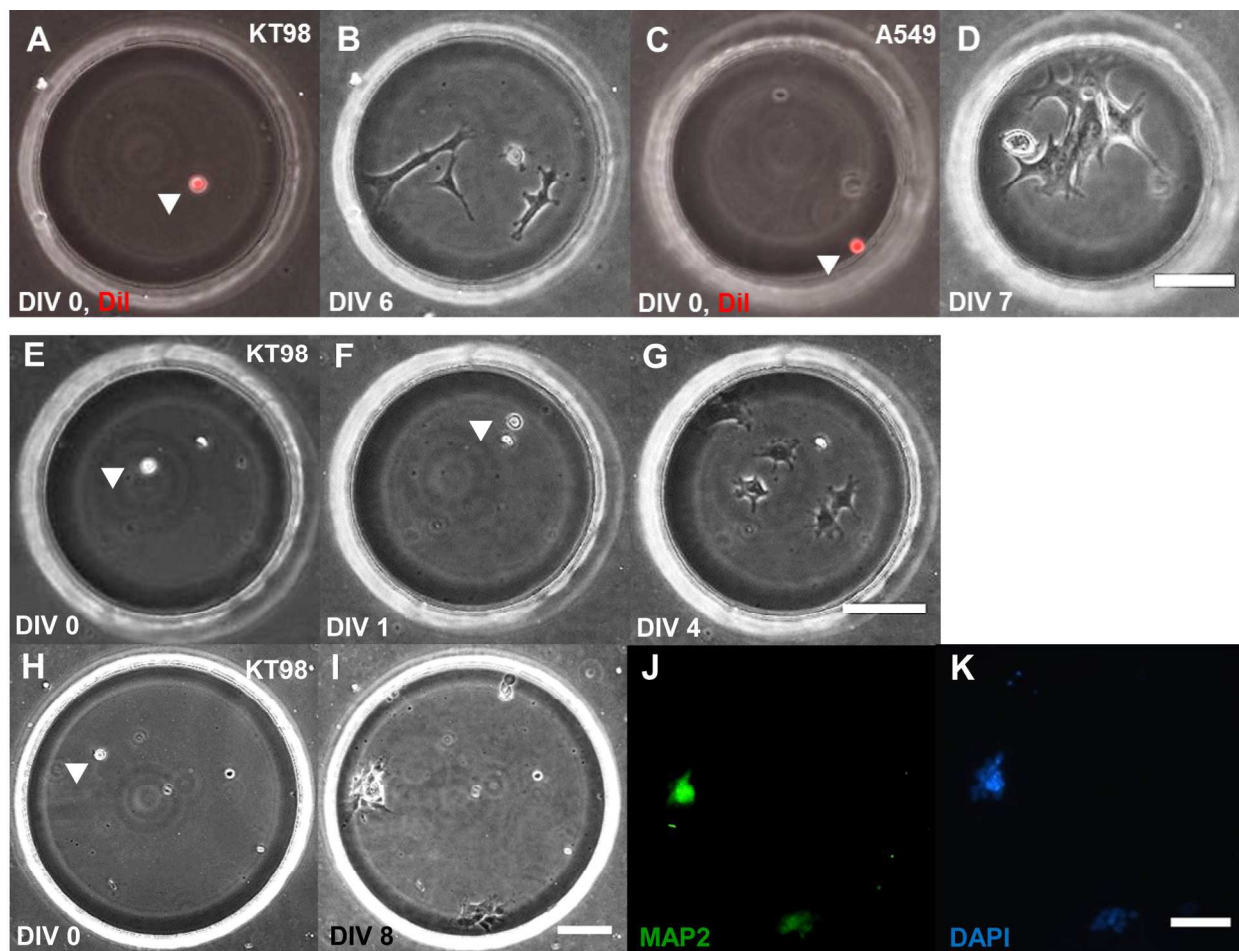


**Figure 6. Cell proliferation and neuronal lineage differentiation of neural stem cell in culture-wells for 6 – 8 days.**

(A) Cell membrane dye (DiI) staining facilitated cell identification shown in phase and fluorescence overlapped image. (B) Proliferated KT98 colony in culture-well after 6 days of *in vitro* culture. (C) DiI staining images showing a single A549 cell loaded in culture-well. (D) Proliferated A549 colony which exhibited normal cell morphology in culture-well after 7 days *in vitro*. Arrowheads indicated the single cells. (E-G) Phase images showing the proliferation

and differentiation of a single KT98 cell in culture-well (285  $\mu\text{m}$  in diameter). The cell divided to 6 cells and exhibited neurite morphology after cultured in differentiation medium for three days. (H-I) A single KT98 cell in culture-well (485  $\mu\text{m}$  in diameter) showing the proliferation and differentiation process from DIV 0 to DIV 8. (J) The differentiated KT98 cells expressed neuronal lineage marker MAP2 after 7 days of differentiation. (K) Cell nucleus were stained with DAPI as the counter staining. Arrowheads indicated single cells in culture-wells. Scale bar: 100  $\mu\text{m}$ .

### Dual-Well device for small molecule testing on colony formation assay

Due to its high single-cell capture efficiency and the large space of culture well, the DW device represents an attractive tool for *in vitro* single-cell colony formation assays in which the growth of individual cells is analyzed. For cancer research, single-cell colony formation assay can be used to test the effect of drugs or small molecules on cancer cell proliferation.

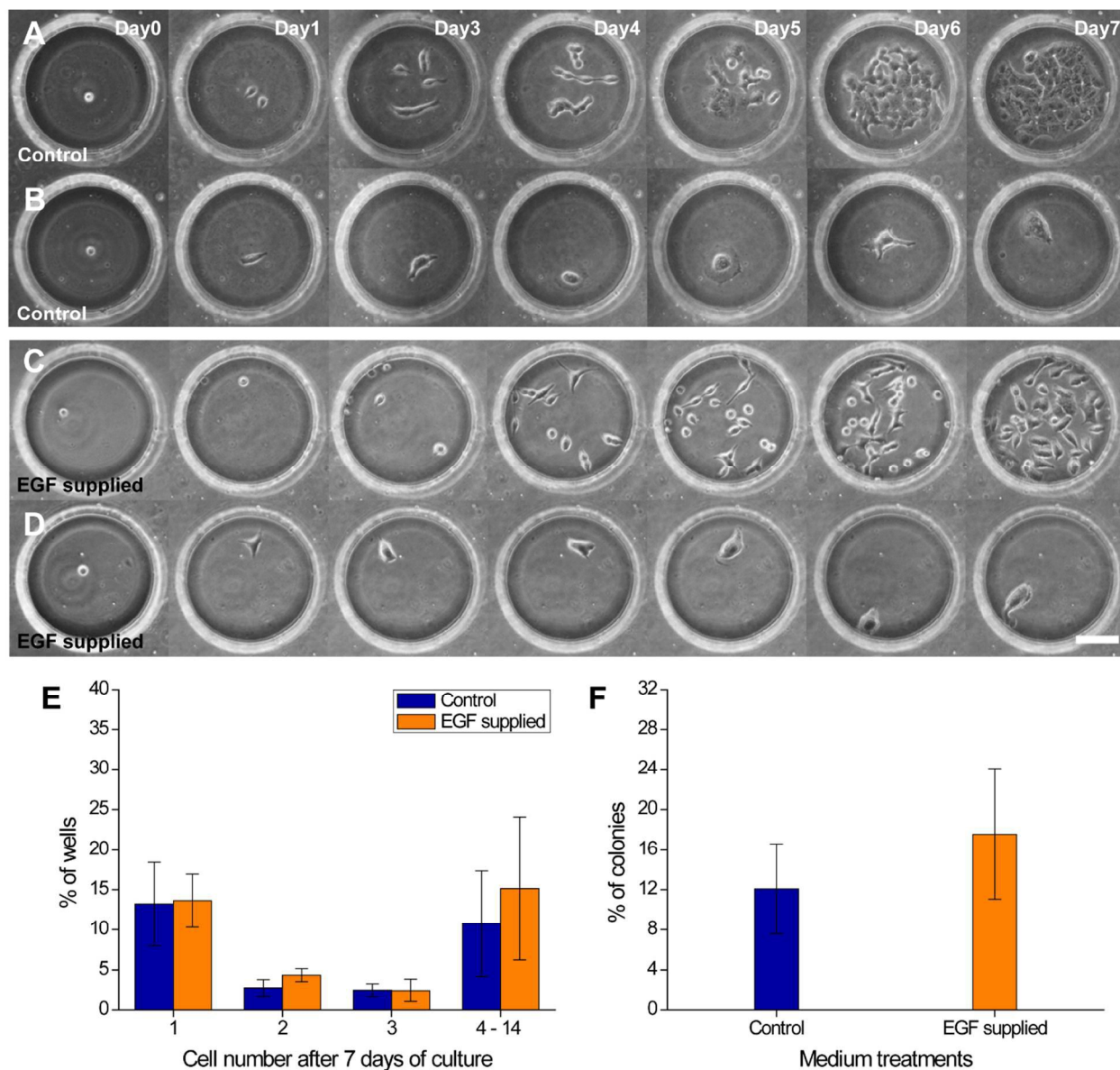
We used A549 cells to test their colony formation abilities in response EGF, which is widely used to study epidermal growth factor receptor-mediated signaling for cancer treatment.

Figure 7F shows that the higher colony forming efficiency (17.56%) was obtained from cells in EGF supplied medium compared to that (12.10%) treated with control medium. Our result confirmed that the EGF-receptor expressing A549 cancer cells proliferate more rapidly when exposed to EGF<sup>42</sup>. Note that the portability and transparency of the DW device allowed the cells in the device to be conveniently analyzed with a conventional microscope during the cell culture experiment (Figure 7A – D). This assay also highlights the strength of the DW device by showing its applicability to studying cellular heterogeneity at the single cell level, as we were able to measure the differences in cell survival and proliferation rate among the tested individual A549 cells. Only 40 – 55% of the loaded cells survived after 7 days of culture, and those live cells exhibited different growth patterns and rates (*e.g.* 1 cell (13%), 2 cells (2.8 –

4.3%), 3 cells (2.5%), and 4 – 14 cells (10 – 15%), Figure 7E). These results demonstrated that the DW device can be used for single-cell colony formation assays, and is advantageous because a large number of individual cell colonies grown in a small area can be straightforwardly measured with a conventional microscope.

5





**Figure 7. Epithelial growth factor (EGF) promoted colony formation ratio of A549 single cells after 7 days of culture.**

(A) A cell colony grew from an A549 single-cell and (B) a single-cell did not proliferate but survived in the control medium treatment after 7 days of culture. (C) Single A549 cell proliferated to form a colony. (D) An undivided single-cell survived for 7 days after culture in

the EGF supplied medium. Scale bar: 100  $\mu\text{m}$ . (E) The A549 single-cells showed a heterogeneous cell number distribution after been cultured in the control or EGF supplied medium for 7 days. (F) The colony forming efficiency of A549 cells with EGF supplied medium was higher than that of the A549 cells cultured with control medium. Each

5 experiment was performed in triplicate.

## Discussion

Single-cell manipulation has been successfully demonstrated with microfabricated systems employing different designs and operation principles,<sup>14, 43-45</sup> among which microwell-based devices are relatively simple and straightforward to design and fabricate making them easily adaptable for different applications.<sup>46</sup> Based on the needs of particular experiments, the well size, number and shape can be tailored for different applications including single hematopoietic stem cell proliferation<sup>30</sup>, individual leukocytes sorting<sup>47</sup>, large-scale single cell trapping<sup>16</sup> and high-throughput drug testing.<sup>48</sup> For applications where long-term culture is needed, using microwells with sizes that are much larger than a single cell is required to provide enough space for cells to attach to the surface and grow. For example, Lecault *et al.* reported a microfluidic device containing large microwells ( $160^3 \mu\text{m}^3$ ) which allowed for hematopoietic stem cell proliferation for 66 hours, however, the efficiency for obtaining a single-cell in a microwell was only 10 – 30%.<sup>30</sup> On the other hand, for applications where maximizing single-cell event is of priority, the microwells were typically made of sizes close to that of a single cell<sup>16</sup>; however they are not able to provide space for cells to spread to their normal morphologies and proliferate. To address this limitation, Park *et al.* designed triangular microwells that have enlarged area for cell growth and were able to achieve 58.34% of PC3

cell trapping rate. However, these microwells were relatively small (with the length of a side ~50  $\mu\text{m}$ ) and thus supported cell proliferation for up to two days<sup>34</sup>. Using our dual-well concept, the efficiency of single-cell loading in large microwells could effectively overcome the Poisson distribution limit (~37%) encountered by limiting dilution methods and open well systems<sup>11</sup>.

From our single-cell loading efficiency study, we found that the number of cell-occupied capture-wells is very close to the number of cell-occupied culture-wells, indicating that most cells could be effectively transferred from captured- to culture-wells. Based on these observation, the efficiency of single-cell loading in culture-wells might be further increased by increasing the efficiency of single-cell loading in the capture-wells, possibly by optimizing the dimensions (i.e., diameter and depth) of the capture-well for specific cell types (Figure 5E) and operation parameters (e.g., cell concentration, sweeping and washing flow rate). Additionally, to know the shear stress exerted on the cells during the washing step, finite element simulation (COMSOL Multiphysics) was used to simulate the wall shear stress of capture-well and microchannel bottom surface in the DW device. We found even at a higher washing flow rate condition of 600  $\mu\text{L}/\text{min}$ , the shear stress on the side-wall of capture-well (ranged from 0 – 0.06 Pa) and bottom surface of the microchannel (0.06 – 0.15 Pa ) (Figure S4)

was very low compared to the physiological wall shear stress in human blood vessels which ranges from 0.5 to 4 Pa depending on the types, sizes and geometries of blood vessels.<sup>49</sup>

Finally in the DW device, the large well size (each ~20 nL) and the microchannel (~60  $\mu$ L) together could provide sufficient medium volume for cells to grow without medium exchange for single-cell colonies culture. For our KT98 and A549 cell proliferation experiments the medium-volume to cell-number ratio was 2 – 3 nL/cell which has allowed the cells to grow for 6 – 7 days and still exhibited normal cell morphology (Figure 8C and 8F). This medium-volume to cell-number ratio is close to the suggested ratio of a commercial low-volume cell culture well plate product (1536 well plate, Corning®, USA). We believe it would be straightforward to use the DW concept for other applications where *in vitro* culture of single cells is required; such as high-throughput drug or toxicity screening<sup>48, 50, 51</sup>, cancer stem cell selection by colony formation,<sup>52</sup> and heterogeneity identification of neural stem cells by neurosphere assay<sup>53</sup>.

## Conclusions

We have presented a new microfluidic single cell-culture device which utilizes a dual-well concept to increase single-cell loading efficiency in micro-wells who sizes are significantly larger than a single cell. We have also demonstrated the use of the DW device in cell differentiation and colony formation assay experiments with cancer and stem cells. We believe that the ability of our approach to allow for high-efficiency loading of single cells in large microwells may be useful for a broad range of applications where on-device culture and analysis of single cells are required.

## ASSOCIATED CONTENT

**Supporting Information**

Additional material as described in the text. This material is available free of charge via the Internet.

## AUTHOR INFORMATION

**Corresponding Author**

\* Corresponding Author:

Chia-Hsien Hsu, Ph.D.

Institute of Biomedical Engineering and Nanomedicine, National Health Research Institutes

35 Keyan Road, Zhunan, Miaoli County 35053, Taiwan

Tel: +886-37-246-166 ext. 37105

Fax: +886-37-586-440

E-mail: [chs@nhri.org.tw](mailto:chs@nhri.org.tw)

Ing-Ming Chiu, Ph. D.

Institute of Cellular and Systems Medicine, National Health Research Institutes

35 Keyan Road, Zhunan, Miaoli County 35053, Taiwan

Tel: +886-37-246-166 ext. 37501

Fax: +886-37-586-440

E-mail: [ingming@nhri.org.tw](mailto:ingming@nhri.org.tw)

#### Funding Sources

This work was supported by a grant from the National Health Research Institutes (03-A1 BNMP11-014).

#### ACKNOWLEDGMENT



## References

1. O. N. Suslov, V. G. Kukekov, T. N. Ignatova and D. A. Steindler, *P Natl Acad Sci USA*, 2002, **99**, 14506-14511.
2. T. Graf and M. Stadtfeld, *Cell Stem Cell*, 2008, **3**, 480-483.
3. M. Shackleton, E. Quintana, E. R. Fearon and S. J. Morrison, *Cell*, 2009, **138**, 822-829.
4. P. Cahan and G. Q. Daley, *Nat Rev Mol Cell Bio*, 2013, **14**, 357-368.
5. H. Clevers, *Nature medicine*, 2011, **17**, 313-319.
6. S. J. Altschuler and L. F. Wu, *Cell*, 2010, **141**, 559-563.
7. D. Di Carlo, H. T. K. Tse and D. R. Gossett, in *Single-Cell Analysis*, Springer, 2012, pp. 1-10.
8. A. Ulloa-Aguirre and P. M. Conn, *Cellular Endocrinology in Health and Disease*, Elsevier, 2014.
9. D. G. Spiller, C. D. Wood, D. A. Rand and M. R. H. White, *Nature*, 2010, **465**, 736-745.
10. L. Vermeulen, M. Todaro, F. D. Mello, M. R. Sprick, K. Kemper, M. P. Alea, D. J. Richel, G. Stassi and J. P. Medema, *P Natl Acad Sci USA*, 2008, **105**, 13427-13432.
11. H. M. Shapiro, *Practical flow cytometry*, John Wiley & Sons, 2005.
12. K. G. Leong, B. E. Wang, L. Johnson and W. Q. Gao, *Nature*, 2008, **456**, 804-808.
13. E. Shapiro, T. Biezuner and S. Linnarsson, *Nat Rev Genet*, 2013, **14**, 618-630.
14. H. B. Yin and D. Marshall, *Curr Opin Biotech*, 2012, **23**, 110-119.
15. C. H. Lin, D. C. Lee, H. C. Chang, I. M. Chiu and C. H. Hsu, *Analytical Chemistry*, 2013, **85**, 11920-11928.
16. J. R. Rettig and A. Folch, *Analytical Chemistry*, 2005, **77**, 5628-5634.
17. J. Clausell-Tormos, D. Lieber, J. C. Baret, A. El-Harrak, O. J. Miller, L. Frenz, J. Blouwolff, K. J. Humphry, S. Koster, H. Duan, C. Holtze, D. A. Weitz, A. D. Griffiths and C. A. Merten, *Chem Biol*, 2008, **15**, 875-875.
18. J. Pan, A. L. Stephenson, E. Kazamia, W. T. Huck, J. S. Dennis, A. G. Smith and C. Abell, *Integrative Biology*, 2011, **3**, 1043-1051.
19. L. S. Jang, P. H. Huang and K. C. Lan, *Biosens Bioelectron*, 2009, **24**, 3637-3644.
20. R. S. Thomas, H. Morgan and N. G. Green, *Lab Chip*, 2009, **9**, 1534-1540.
21. D. Di Carlo, N. Aghdam and L. P. Lee, *Analytical Chemistry*, 2006, **78**, 4925-4930.
22. H. Y. Chen, J. Sun, E. Wolvetang and J. Cooper-White, *Lab Chip*, 2015, **15**, 1072-1083.
23. N. Klauke, G. L. Smith and J. Cooper, *Biophys J*, 2003, **85**, 1766-1774.

24. N. Klauke, P. Monaghan, G. Sinclair, M. Padgett and J. Cooper, *Lab Chip*, 2006, **6**, 788-793.
25. D. Wlodkowic, S. Faley, M. Zagnoni, J. P. Wikswo and J. M. Cooper, *Analytical Chemistry*, 2009, **81**, 5517-5523.
26. S. Gabriele, M. Versaevel, P. Preira and O. Theodoly, *Lab Chip*, 2010, **10**, 1459-1467.
27. N. Jokilaakso, E. Salm, A. Chen, L. Millet, C. D. Guevara, B. Dorvel, B. Reddy, A. E. Karlstrom, Y. Chen, H. M. Ji, Y. Chen, R. Sooryakumar and R. Bashir, *Lab Chip*, 2013, **13**, 336-339.
28. A. Revzin, R. G. Tompkins and M. Toner, *Langmuir*, 2003, **19**, 9855-9862.
29. S. Lindstrom, M. Eriksson, T. Vazin, J. Sandberg, J. Lundeborg, J. Frisen and H. Andersson-Svahn, *PloS one*, 2009, **4**, e6997.
30. V. Lecault, M. VanInsberghe, S. Sekulovic, D. J. H. F. Knapp, S. Wohrer, W. Bowden, F. Viel, T. McLaughlin, A. Jarandehi, M. Miller, D. Falconnet, A. K. White, D. G. Kent, M. R. Copley, F. Taghipour, C. J. Eaves, R. K. Humphries, J. M. Piret and C. L. Hansen, *Nat Methods*, 2011, **8**, 581-593.
31. V. I. Chin, P. Taupin, S. Sanga, J. Scheel, F. H. Gage and S. N. Bhatia, *Biotechnol Bioeng*, 2004, **88**, 399-415.
32. M. Charnley, M. Textor, A. Khademhosseini and M. P. Lutolf, *Integrative Biology*, 2009, **1**, 625-634.
33. J. C. Liu, T. Deng, R. S. Lehal, J. Kim and E. Zacksenhaus, *Cancer Res*, 2007, **67**, 8671-8681.
34. J. Y. Park, M. Morgan, A. N. Sachs, J. Samorezov, R. Teller, Y. Shen, K. J. Pienta and S. Takayama, *Microfluid Nanofluid*, 2010, **8**, 263-268.
35. D. B. Wolfe, D. Qin and G. M. Whitesides, *Methods Mol Biol*, 2010, **583**, 81-107.
36. P. C. Li, *Microfluidic lab-on-a-chip for chemical and biological analysis and discovery*, CRC press, 2010.
37. Y. C. Hsu, D. C. Lee, S. L. Chen, W. C. Liao, J. W. Lin, W. T. Chiu and I. M. Chiu, *Dev Dyn*, 2009, **238**, 302-314.
38. S. Yamamura, H. Kishi, Y. Tokimitsu, S. Kondo, R. Honda, S. R. Rao, M. Omori, E. Tamiya and A. Muraguchi, *Analytical Chemistry*, 2005, **77**, 8050-8056.
39. A. Soto-Gutierrez, N. Navarro-Alvarez, D. Zhao, J. D. Rivas-Carrillo, J. Lebkowski, N. Tanaka, I. J. Fox and N. Kobayashi, *Nat Protoc*, 2007, **2**, 347-356.
40. B. Y. Hu, Z. W. Du and S. C. Zhang, *Nat Protoc*, 2009, **4**, 1614-1622.
41. A. Chojnacki and S. Weiss, *Nat Protoc*, 2008, **3**, 935-940.
42. S. Tracy, T. Mukohara, M. Hansen, M. Meyerson, B. E. Johnson and P. A. Janne,

- Cancer Res*, 2004, **64**, 7241-7244.
43. C. H. Hsu, C. C. Chen and A. Folch, *Lab Chip*, 2004, **4**, 420-424.
  44. L. Mazutis, J. Gilbert, W. L. Ung, D. A. Weitz, A. D. Griffiths and J. A. Heyman, *Nat Protoc*, 2013, **8**, 870-891.
  45. T. A. Nguyen, T. I. Yin, D. Reyes and G. A. Urban, *Analytical Chemistry*, 2013, **85**, 11068-11076.
  46. S. Lindstrom and H. Andersson-Svahn, *Bba-Gen Subjects*, 2011, **1810**, 308-316.
  47. A. Revzin, K. Sekine, A. Sin, R. G. Tompkins and M. Toner, *Lab Chip*, 2005, **5**, 30-37.
  48. P. C. Chen, Y. Y. Huang and J. L. Juang, *Lab Chip*, 2011, **11**, 3619-3625.
  49. W. V. Potters, H. A. Marquering, E. VanBavel and A. J. Nederveen, *Current Cardiovascular Imaging Reports*, 2014, **7**, 1-12.
  50. T. Tanaka, S. Tohyama, M. Murata, F. Nomura, T. Kaneko, H. Chen, F. Hattori, T. Egashira, T. Seki, Y. Ohno, U. Koshimizu, S. Yuasa, S. Ogawa, S. Yamanaka, K. Yasuda and K. Fukuda, *Biochem Bioph Res Co*, 2009, **385**, 497-502.
  51. P. Liang, F. Lan, A. S. Lee, T. Y. Gong, V. Sanchez-Freire, Y. M. Wang, S. Diecke, K. Sallam, J. W. Knowles, P. J. Wang, P. K. Nguyen, D. M. Bers, R. C. Robbins and J. C. Wu, *Circulation*, 2013, **127**, 1677-1691.
  52. V. Tirino, V. Desiderio, F. Paino, A. De Rosa, F. Papaccio, M. La Noce, L. Laino, F. De Francesco and G. Papaccio, *Faseb J*, 2013, **27**, 13-24.
  53. M. Cordey, M. Limacher, S. Kobel, V. Taylor and M. P. Lutolf, *Stem Cells*, 2008, **26**, 2586-2594.